Journal of Energy

VOLUME 63 Number 1–4 | 2014 Special Issue

journal homepage: http://journalofenergy.com/

Bruno Bošnjak
Siemens AG Power Transformers Nürnberg
bruno.bosnjak@siemens.com

Mario Stuhne
Končar - Power Transformers Ltd.
mario.stuhne@siemens.com

ANALYSIS AND EXPERIMENTAL VERIFICATION OF STATIC TILTING BEHAVIOUR OF CTC IN TRANSFORMER WINDINGS

SUMMARY

This paper presents a numerical model and experimental verification of the critical tilting force calculation for transformer winding conductors under static axial pressure. For the purposes of this investigation a structural finite element method model of a non-epoxy bonded continuously transposed conductor used for the construction of transformer windings was developed. The mechanical behaviour of two different transformer winding conductors under static axial pressure was simulated. The radial position of CTCs was varied according to manufacturer tolerances in order to closer correspond to the actual physical models. The displacements, stresses and strains obtained from the simulation are presented and analysed. This calculation is compared to existing analytical and empirical calculations in the IEC 60076-5:2006 and available literature. The results of these calculations were experimentally checked by pressing three physical winding models in a hydraulic press with the force corresponding to calculated critical tilting force and above. The resulting deformations of the winding conductors were photographed and compared to the results of the simulations.

Key words: Transformer, Windings, Short Circuit, Tilting, FEM, Structural Simulation

1. INTRODUCTION

Transformer windings consisting of current-carrying conductors are situated in the stray magnetic flux in the transformer window. Due to the interaction of the time-varying magnetic field and current flowing through the winding conductors, Lorentz forces are generated that act on the winding conductors. During a short circuit, if the axial compression exceeds a certain limit, a failure mode called tilting may occur which tilts the conductors of disk windings in a specific zig-zag pattern. This type of failure can damage the winding insulation, induce even higher forces due to conductor displacement and cause inter-turn short-circuits [1]. Currently, the calculation of the critical axial force under which tilting occurs is limited to analytical [2][3][4] and semi-empirical approaches [5]. This paper introduces a 2D finite element method calculation of stresses and corresponding displacements that occur during the pressing of two continuously transposed conductors (CTCs). The results of this calculation are compared to existing analytical calculations as well as to the experimental results. Primary object of this investigation was the characterisation of the mechanical behaviour of strandwise tilting [4].

2. EXISTING CALCULATIONS OF CRITICAL TILTING FORCE

2.1. Theoretical calculation approach

Current analytical calculations are primarily concerned with the calculation of the critical axial force under which tilting occurs. From [3], the following equation is available for the calculation of the critical axial force under which tilting occurs:

$$F_{tilt1} = \frac{4}{3} E_0 \left[\frac{a_n \cdot \pi \cdot h_1^2}{D_{mean}} \frac{\left[1 + \frac{b_1^2}{h_1^2}\right] \cdot D_{mean}^2}{4 \cdot L \cdot l_c \cdot (1+\mu)} - \frac{l_c}{L} + \frac{1}{4} \right] \cdot 10^{-3} [\mathrm{kN}] \tag{1}$$

where

E_0	- Young's modulus of elasticity for copper 113000 [N/mm^2]
a_n	- width of the winding [mm]
h_1	- height of the CTC strand [mm]
b_1	- width of the CTC strand [mm]
D_{mean}	- mean winding diameter [mm]
L	- transposition distance in which one full transposition of all strands is completed [mm]
l_c	- distance over which one strand is transposed from one position to another [mm]
μ	- Poisson's ratio for copper

This analysis considers a winding made up of CTCs under the influence of an axial force from a theoretical standpoint, but does not take into account the additional complexities of the transformer winding geometry such as axial spacers, interaction between discs and material properties of paper and pressboard.

2.2. Semi-empirical calculation approach

IEC standard 60076-5 [5] prescribes the following equation for the calculation of the critical axial force under which tilting occurs:

$$F_{tilt2} = \left[\frac{E_0}{2} \cdot \frac{n_r \cdot b_1 \cdot h_1^2}{D_{mean}} + K_2 \frac{n_r \cdot X \cdot \pi \cdot b_1^3 \cdot D_{mean} \cdot \gamma}{h_1} \right] \cdot K_3 \cdot K_4 \cdot 10^{-3} [\mathrm{kN}] \tag{2}$$

where

n_r	- number of strands or twin conductors in the winding radial width
K_2	- coefficient for the bedding term, 22 for non-bonded CTC [N/mm^3]
X	- spacer coverage factor for disc- and helical-type windings $X = \frac{c \cdot z}{\pi \cdot D_{mean}}$
c	- radial spacer width [mm]
z	- number of radial spacers around the circumference
γ	- conductor shape constant; 1,0 for standard corner radius, 0,85 for fully rounded strands
K_3	- factor accounting for the copper work hardening degree (see Table I)
K_4	- factor accounting for dynamic tilting

Table I – Values for factor K_3

$R_{p0.2}$ MPa	K_3
Annealed	1.0
150	1.1
180	1.2
230	1.3
>230	1.4

Table II – Values for factor K_4

Conductor type	Winding type	
	Disc - helical	Layer
Strand or twin	1.2	1.1
Non-bonded CTC	1.7	1.3

For the purposes of this paper, the critical tilting forces were calculated with the dynamic tilting factor set at 1.0. This equation is based on a semi-empirical approach, stemming from theoretical considerations and statistical data.

2.3. Winding conductor data

Both analytical and numerical calculations were performed on the two types of continuously transposed conductor available. Experimental verification was performed on three winding models:

a) Model 1 Winding
b) Model 2 Winding
c) Model 3 Winding – modified Model 2 winding with one less conductor in the radial direction in the top most disc

The basic data of each winding model is presented in the following table.

Table III – Winding and conductor model data

Model	Winding type	Spacers	n_{rad}	n_{CTC}	h_1	b_1	δ_{laq}	n_{paper}
Model 1	Disc winding	No	8	15	4,85	1,4	0,1	12
Model 2	Disc winding	Yes	3	47	9,05	1,42	0,1	6
Model 3	Disc winding	Yes	2	47	9,05	1,42	0,1	6

where

n_{rad} - number of CTCs in the winding radially

n_{CTC} - number of CTC strands

δ_{laq} - thickness of the varnish layer

n_{paper} - number of paper layers on the conductor

2.4. Analytical calculation results

Using equations (1) and (2), the following values of critical tilting force were calculated:

Table IV – Calculated critical titling forces

Model	F_{tilt1} [kN] Theoretical	F_{tilt2} [kN] Semiempiric
Model 1	2435	3880
Model 2	3218	1242
Model 3	2124	822

3. NUMERICAL MODEL OF THE CONDUCTORS

The two conductor models, corresponding to the two types of conductor used in the calculations and the experimental verifications were modelled and solved using ANSYS R15.0 Workbench environment. Models are shown in Figure 1 and Figure 2.

Models developed were axially symmetric, with a force applied to structure at the top of the model which was modelled as a transformerboard object. Applied force had the amplitude of 2542 kN, which is the maximal pressing force applied in the consequent experiment.

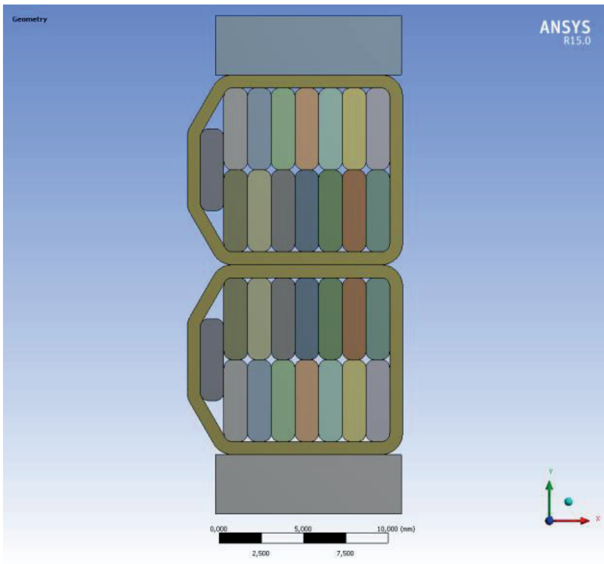

Figure 1 – Model 1 conductor geometry

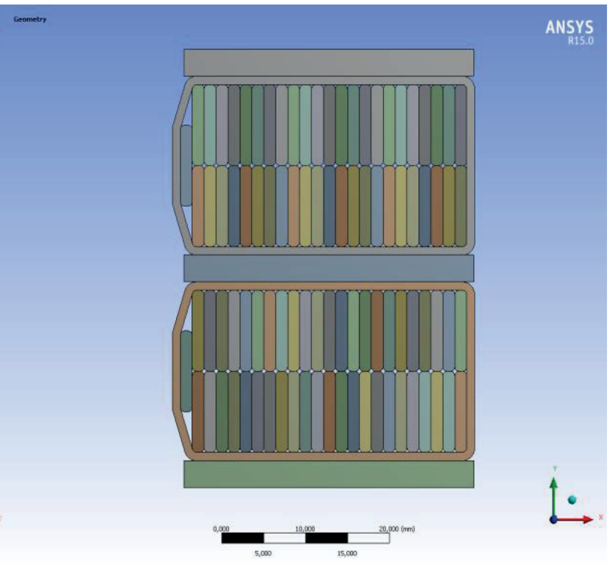

Figure 2 – Model 2 and 3 conductor geometry

Two additional conductor models were developed with a built-in horizontal offset of the CTC strands by 0.2mm according to the tolerances of conductor manufacturer. These models are shown in Figure 3 and Figure 4.

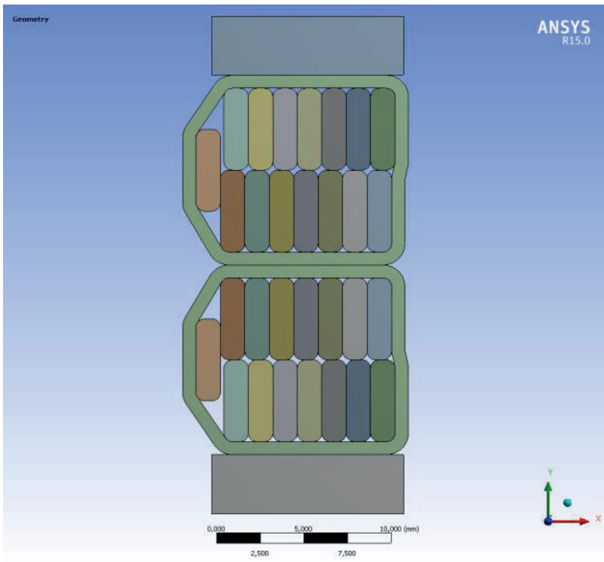

Figure 3 – Model 1 conductor geometry with a 0.2 mm horizontal offset

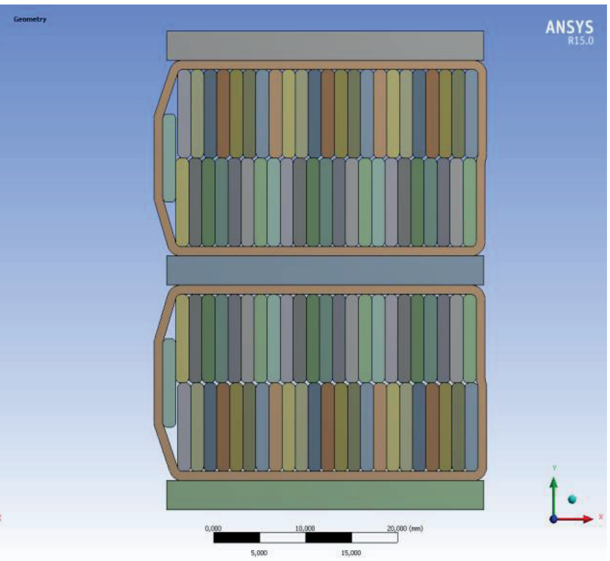

Figure 4 - Model 2 and 3 conductor geometry with a 0.2mm horizontal offset

4. SIMULATION RESULTS

The results of the static structural simulation are presented in the following figures. Displacement and stress are plotted for the both the case with perfect alignment and 0.2mm horizontal offset.

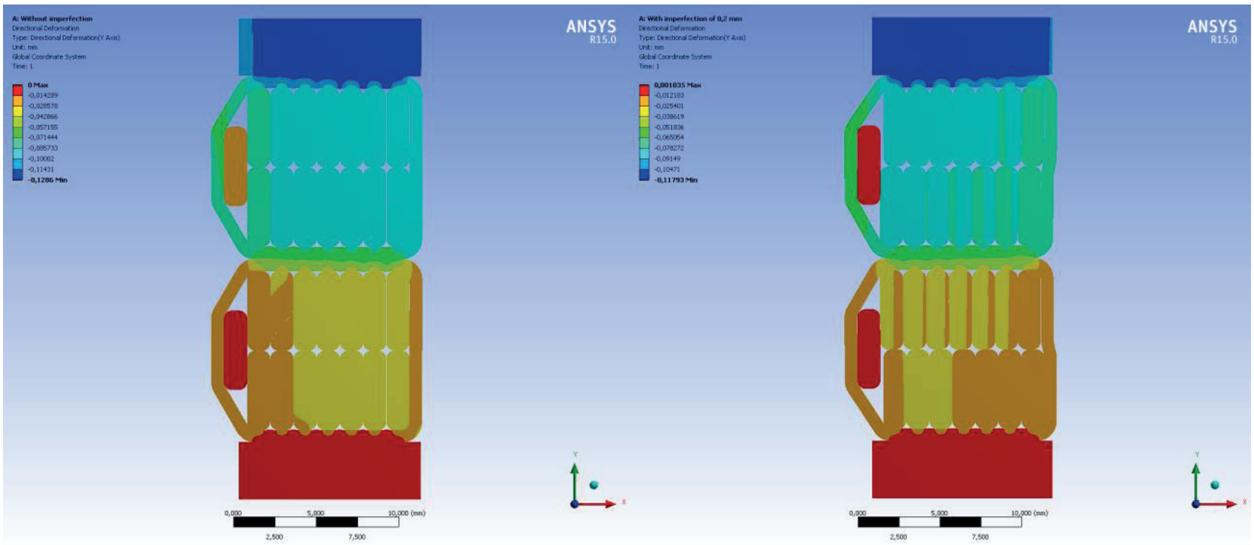

a) Perfect alignment of strands **b) 0.2mm horizontal offset**

Figure 5 – Vertical displacement (y-axis) plots Model 1

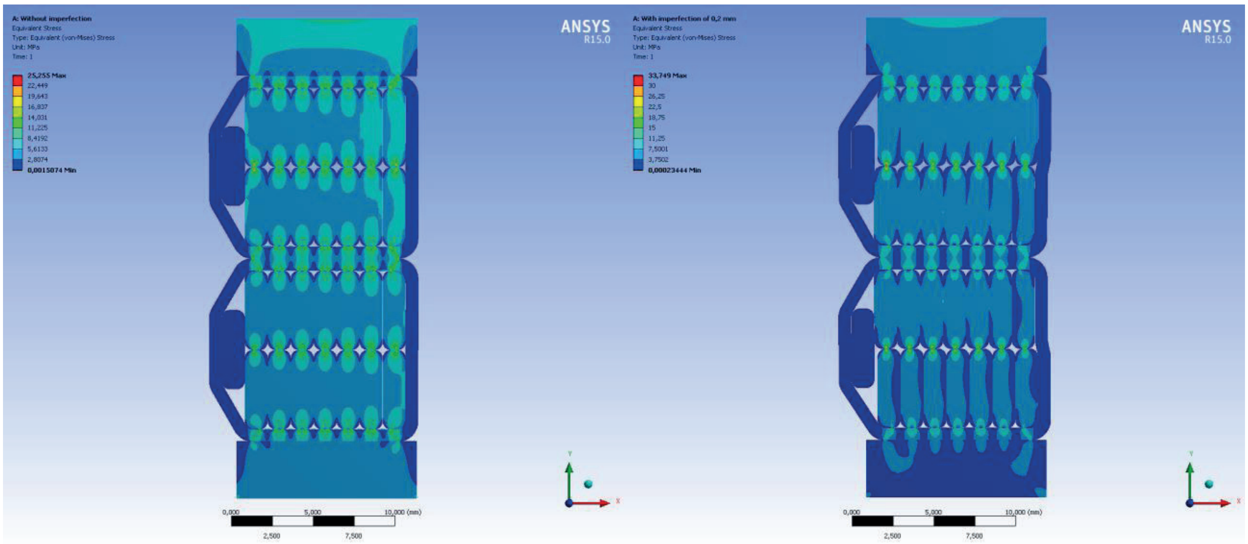

a) Perfect alignment of strands **b) 0.2mm horizontal offset**

Figure 6 – Stress plots Model 1

The vertical displacement plot of Model 1 in Figure 5 shows the tendency of the top-most conductor to have the higher vertical displacements, i.e. the top most conductor experience the highest compression. Introduction of a 0.2 mm horizontal offset to the two conductor strand rows in Model 1 increases the maximum stress experienced by the conductor strands from 25,2 MPa to 33,7 MPa and changes the distribution of stress within the strands into a pattern more similar to the expected titling stress patterns (Figure 6). Although the stress within the conductor is higher, the vertical displacement of the conductors is lower for the case with 0.2 mm offset. The 0.2 mm offset effectively causes the “wedging” of the conductor strands into one another to a certain degree, locking them into place. Therefore, in spite of higher maximum stress experienced in the contact points between the conductors, the average stress in each conductor strand is in fact lower when a 0.2 mm offset is present than when the conductor strands are perfectly aligned.

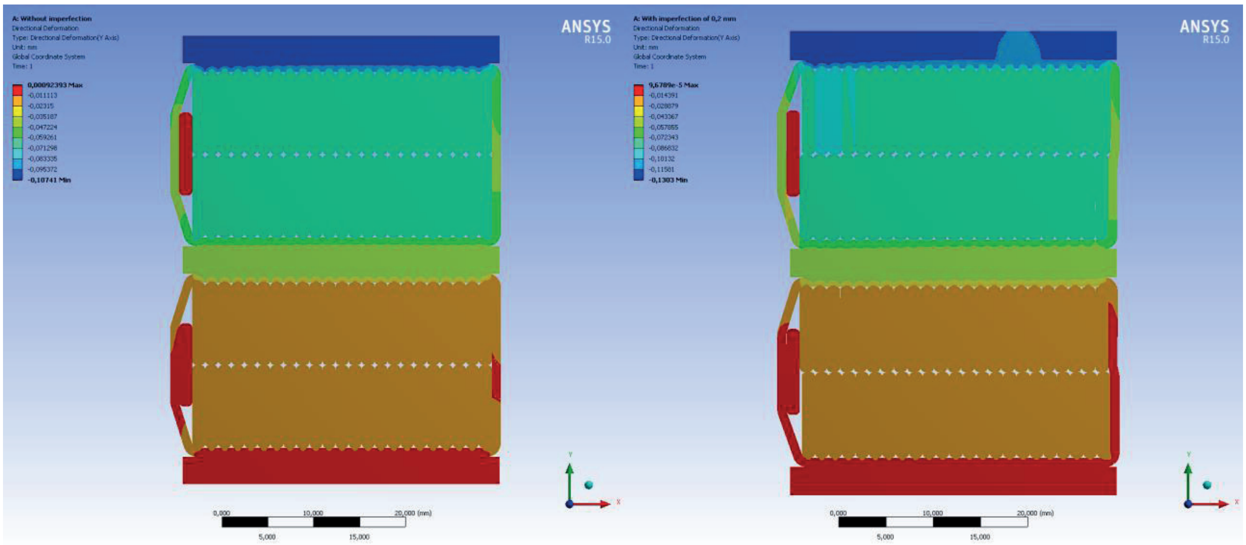

a) Perfect alignment of strands **b) 0,2mm horizontal offset**

Figure 7 – Vertical displacement (y-axis) plots Model 2 and 3

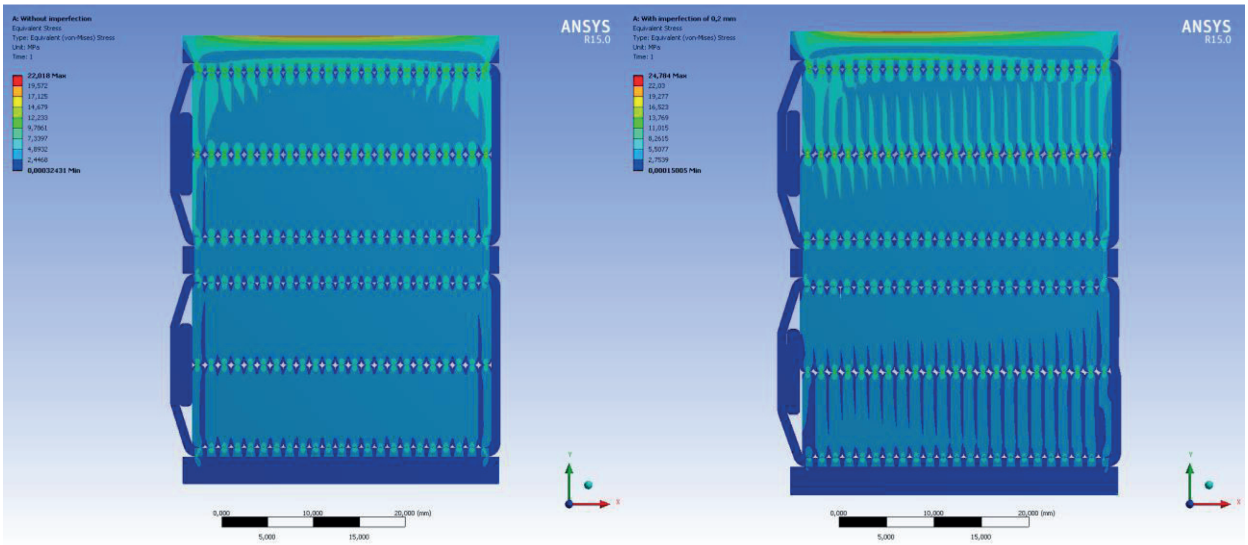

a) Perfect alignment of strands **b) 0,2mm horizontal offset**

Figure 8 – Stress plots Model 2 and 3

The simulation on conductor of Model 2 and 3 shows a similar general pattern of behaviour to the Model 1 regarding stress and displacement. The differences stem from the slenderer conductor strands and the higher number of strands overall. The higher number of strands means the maximum stress is lower and the overall distribution of stress and displacement is more even than for the Model 1. Also, no “wedging” effect is present and the vertical displacements are higher for the model with 0.2mm displacement which was the expected results. The equations (1) and (2), according to Table IV, give contradictory results in regards to the tilting withstand capacity of this conductor. The numerical calculation yields results that are more line with the theoretical calculation from [2], i.e. equation (1).

These results indicate that the applied force of 2542 kN will not cause any observable tilting of either conductor used in the experiment, since the maximum displacement is in the 0.1 mm range.

Calculation of the critical tilting force for both winding models was performed for the models with the 0.2 mm horizontal offset of the CTC strands. For Model 1 conductor, critical tilting force was calculated to be at 4016 kN, or 103% of the calculated critical tilting force according to IEC (Table IV).

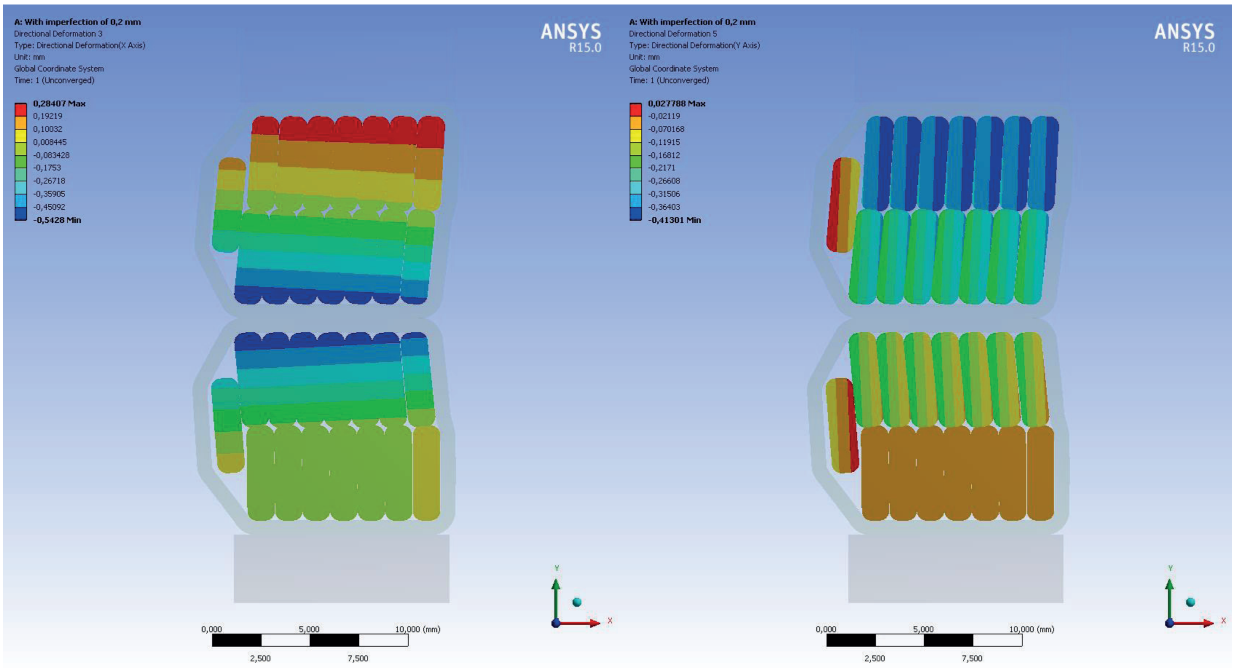

a) Horizontal displacement (x-asis) **b) Vertical displacement (y-axis)**

Figure 9 – Displacement plots for Model 1 winding conductor under 103% of the critical tilting pressing force according to IEC

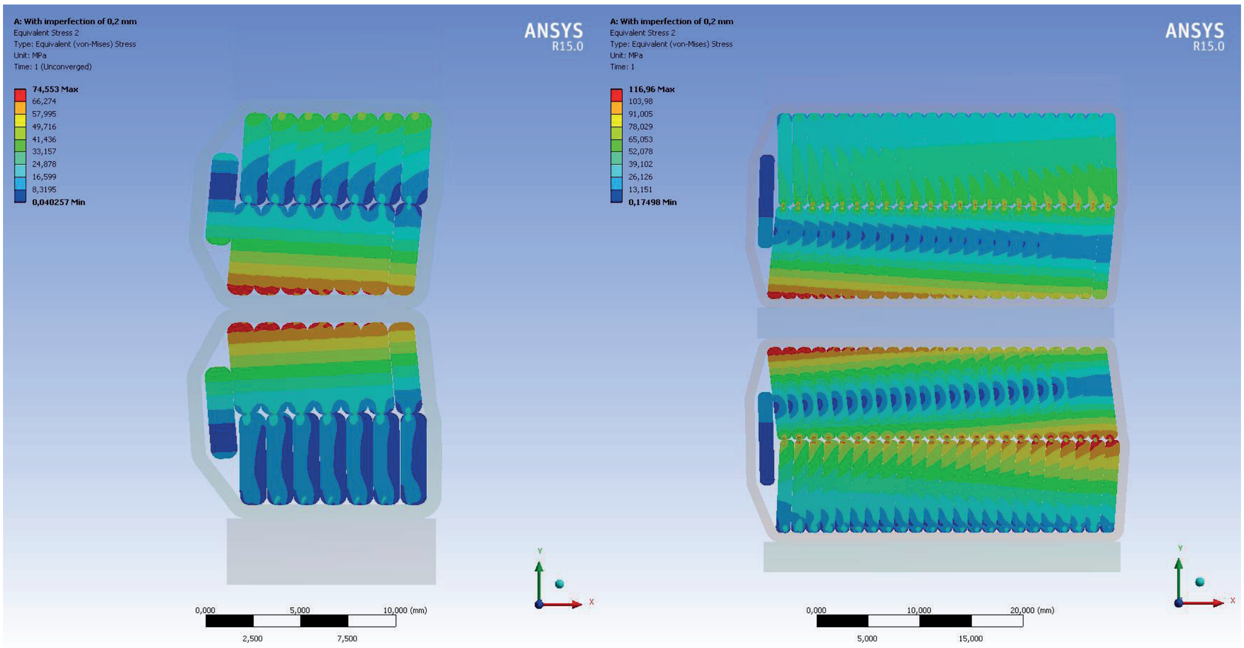

Model 1 under 103% critical tilting force **Model 2 under 614% critical tilting force**

Figure 10 – Stress plots for Models 1 and 2

Model 2 proved to be theoretically very resistant to tilting, as a complete tilt of the conductor was not achieved even at the force of 7626 kN which amounts 614% to of the critical tilting force according to IEC for Model 2 and 927% of the critical tilting force according to IEC for Model 3.

5. EXPERIMENTAL VERIFICATION

All three winding models were pressed using a hydraulic press with forces amounting to 50% and 100% critical tilting force according to IEC Standard 60076-5[5], calculated using the equation (2). For Model 1, since the 100% tilting force was at calculated at 3880 kN, the maximum allowed pressing forces were applied, amounting to 65% of the critical tilting force. The calculation results are presented in Table IV. All three winding models also were pressed using the maximum pressing force allowed on the hydraulic press due to safety regulation in the amount of 2542 kN. When subjected to 50% and 100% of the critical tilting force according to IEC Standard 60076-5, Model 2 and 3 exhibited no visible deformations of the copper conductors, even after a prolonged pressing time of 1 hour. The only visible deformation was the impressing of insulation paper into the radial spacers on Model 3 shown in Figure 11.

Figure 11 –Model 3 under the influence of the 100% of the critical tilting pressing force according to IEC

Under the influence of the maximum pressing force allowed on the hydraulic press (2542 kN, 309% of the IEC critical tilting force), visual deformations appeared on the winding conductors. The observed deformations were of within the elastic area of deformations, i.e. after the experiment, when the winding model was released from the press, they retained their previous state of mechanical stability. The winding conductors deformed in the shape precluding tilting, with the top conductor obviously under higher strain than the conductors below it (Figure 12).

Figure 12 – Model 3 under the influence of the 309% of the critical tilting pressing force according to IEC

The winding conductors exhibited an elastic deformation where the conductor strands were rotated around the axial axis of the winding in manner similar to tilting (Figure 13). Therefore, it is safe to assume that under the influence of higher force the winding model would plastically deform in the shape of tilting. The displacements observed were in the 1-4 mm range in the radial direction, which is an order of magnitude greater that the displacements predicted by the numerical simulation. The simulation correctly predicted the shape of the deformation. It is important to note the winding deformed in full-tilt mode [6].

Figure 13 – Model 3 under the influence of the 309%% of the critical tilting pressing force according to IEC

Table V – Experiment with 50% of the critical tilting force applied

Model	F_{tilt2} [kN] Calculation according to [5]	F_{tilt1l} [kN] Calculation according to [3]	F_{tilt13} [kN] Numerical calculation	F_{app} [kN] Applied Force	$\frac{F_{app}}{F_{tilt2}} \cdot 100$ [%]	Observed deformations of the copper conductors
Model 1	3880	2435	4016	1940	50%	No visible deformations
Model 2	1242	3218	>7626	621	50%	No visible deformations
Model 3	822	2124	>7626	411	50%	No visible deformations

Table VI – Experiment with 100% of the critical tilting force applied

Model	F_{tilt2} [kN] Calculation according to [5]	F_{tilt1} [kN] Calculation according to [3]	F_{tilt1l} [kN] Numerical calculation	F_{tilt3} [kN] Numerical calculation	F_{app} [kN] Applied Force	$\frac{F_{app}}{F_{tilt2}} \cdot 100$ [%]	Observed deformations of the copper conductors
Model 1	3880	2435	4016	4016	2542	65%	„Elastic“ tilting 1-2 mm
Model 2	1242	3218	>7626	>7626	1242	100%	No visible deformations
Model 3	822	2124	>7626	>7626	822	100%	No visible deformations

Table VII – Experiment with the maximum allowable force applied

Model	F_{tilt2} [kN] Calculation according to [5]	F_{tilt1} [kN] Calculation according to [3]	F_{app} [kN] Applied Force	F_{tilt3} [kN] Numerical calculation	$\frac{F_{app}}{F_{tilt2}} \cdot 100$ [%]	Observed deformations of the copper conductors
Model 1	3880	2435	2542	4016	65%	„Elastic“ tilting 1-2 mm
Model 2	1242	3218	2542	>7626	204%	„Elastic“ tilting 3-4 mm
Model 3	822	2124	2542	>7626	309%	„Elastic“ tilting 3-4 mm

6. CONCLUSION

The application of numerical calculation for the description of the behaviour of continuously transposed conductor provides a deeper insight into this type of loss of structural stability and enables the calculation of stress within the conductors and the corresponding displacements. Compared to analytical calculations, the numerical model was able to predict the deformation of the conductor under constant force more accurately. Although the 2D numerical model accurately predicted the shape of the deformation, it did not accurately predict the order of magnitude of the displacements observed in the experiment due to the model simplifications. Further research should be performed into more detailed 3D models containing all the details of winding geometry for a more precise prediction of the conductor behaviour under the influence of static forces.

REFERENCES

[1] G. Bertagnolli, "Short-Circuit Duty of Power Transformers - The ABB Approach", 1st ed., Golinelli Industrie Grafiche, January 1996

[2] M. R. Patel, "Dynamic stability of helical and barrel coils in transformers against axial short-circuit forces," Proc. Inst. Elect. Eng., vol. 127, no. 5, Sep. 1980, pp. 281–284.

[3] M. R. Patel „Instability of the Continuously Transposed Cable Under Axial Short-Circuit Forces in Transformers", IEEE Transactions on Power Delivery, Vol. 17, IEEE Power & Energy Society, January, 2002.

[4] A. Bakshi, S. Kulkarni, „Eigenvalue Analysis for Investigation of Tilting of Transformer Winding Conductors Under Axial Short-Circuit Forces", IEEE Transactions on Power Delivery, Vol. 26, No. 4, IEEE Power & Energy Society, Toronto, Canada, October 2011

[5] IEC 60076-5 Power Transformers – Part 5: Ability to withstand short circuit, February 2006

[6] S. V. Kulkarni, S.Khaparde, "Transformer Engineering: Design and Practice", 3rd ed.,Marcel Dekker, 2004